Understanding flame extinction in timber under external heating using high-activation energy asymptotics

Juan I. Cuevas[1,*], Augustin Guibaud[2], Cristian Maluk[1] and José L. Torero[2]

[1] School of Civil Engineering, The University of Queensland, Brisbane, QLD 4072, Australia

[2] Department of Civil, Environmental and Geomatic Engineering, University College London, London, WC1E 6BT, United Kingdom

* Corresponding Author information:

Email address	j.cuevas@uq.edu.au
Full postal address	School of Civil Engineering, Level 5, Advanced Engineering Build., Staff House Rd. St. Lucia Campus, The University of Queensland Brisbane, QLD, 4072, Australia

Abstract

The present study analyses the flaming extinction of timber under different levels of external heating and a range of diluted oxygen contents in the gas phase. An existing theoretical framework conceived initially for the analysis of a counter-flow diffusion flame established above the surface of a condensed fuel is extended for charring materials to deliver a fundamental understanding of the self-extinction of timber. This study shows that the energy balance at the burning surface is influenced primarily by the magnitude of external heating conditions, which directly influences the evolution of bulk properties such as flame temperature, location, and stagnation plane position. Variations in the oxygen content had a lesser influence over these bulk properties. For all investigated conditions, the limits of the strain rates range where a flame can be sustained was shown to vary substantially, and critical Damköhler number (Da) analyses were conducted. Blow-off at high strain rates (low Da) occurs for all investigated conditions. The value of this critical Da decreases when increasing either the magnitude of the external heating or the oxygen content as flame temperature increases. Quenching at low strain rates (high Da) is only found for sufficiently low magnitudes of external heating. There, the associated critical Da increases when increasing either the external heating or the oxygen content. Above a certain degree of external heating, the flame can be theoretically sustained even at infinitely low strain rates. By comparing these results to experimental data, the experimental critical Da at quenching was found to behave like the theoretical results but with a lower sensitivity to variations in the parameters studied. To account for this discrepancy, a fuel dilution parameter is introduced to incorporate the complex dependencies of timber decomposition and surface reactions not captured by the theoretical framework.

Keywords

Flame extinction, timber, counter-flow, Damköhler number, asymptotic analysis

Nomenclature

Symbols

a_1, a_2	Integration constants in the frozen region temperature distribution
B	Pre-exponential factor
c_p	Specific heat capacity (J/kg/K)
D	Binary diffusion coefficient (m/s^2)
Da	Damköhler number (-)
q_c, q_v	Heat of reaction (combustion/pyrolysis) (J)
E	Activation energy (J)
k	strain rate (s^{-1})
$\dot{m}_i''$	Mass flow of species i per unit area (kg/s m^2)
$\dot{q}''$	Heat flux per unit area (W/m^2)
R	Universal gas constant (J/K/mol)
R_a	Ratio of the radiative exchange to the diffusion rate (-)
T	Temperature (K)
t	Time (s)
W_i	Molecular weight of species i (g/mol)
x	Distance (m)
Y	Mass fraction (-)

Subscripts and superscripts

$\sim$	Non-dimensional variable
∞	At infinity, ambient
b	Blow-off extinction
ch	Char, char layer, char oxidation
E	Extinction
exp	Experimental
ext	External
F	Fuel
f	Flame

$_I$	Inert
$_{in}$	In-depth
$_{loss}$	Loss
$_{ox}$	Oxidizer
$_P$	Pyrolysis
$_q$	Quenching extinction
$_s$	Surface
$_{st}$	Stored
$_{theo}$	Theoretical

Greek letters

ε	Small parameter of expansion (-)
λ	Thermal conductivity (W/m/K)
μ	Emissivity (-)
ν_i	Stoichiometric coefficient of species i (-)
ρ	Density (kg/m^3)
σ	Stefan-Boltzmann constant (W/m^2/K^4)
Ψ	Pureness of the pyrolysis gases (-)
Ω	Heat exchange parameter (-)

1 Introduction

As timber burns, a thermal wave propagates through the solid and promotes a series of thermal decomposition processes, the most important being pyrolysis [1]. Pyrolysis reactions are endothermic and are responsible for the generation of flammable gases supplied to the flame. The progression of the pyrolysis front through the material leaves behind a growing layer of a solid residue known as char [2]. Due to its low thermal conductivity, char acts as an insulation barrier that regulates the amount of energy delivered to the pyrolysis front, decreasing the flow of pyrolysis gases being released [3]. In time, reducing the fuel available in the gas phase leads to a decrease in both flame length [4,5], flame temperature, and the heat feedback between the flame and the burning solid.

In the absence of additional heat sources, the rate of energy that is delivered to the pyrolysis front will eventually decrease to a critical point at which the flow of combustible gases being supplied to the flame is not enough to sustain the combustion processes, and flame extinction by quenching follows. This phenomenon is known as the self-extinction of timber, and it plays a crucial role in enabling the safe use of timber for structures in mid and high-rise construction.

Current work focused on determining the set of threshold conditions under which timber self-extinguishes spans across scales. Nevertheless, most of the research work consists of bench-scale experimental studies. Within this context, the works of Emberley *et al.* [6], Bartlett *et al.* [7], Crielaard *et al.* [8], and more recently, Cuevas *et al.* [9] have delivered critical conditions for self-extinction. These conditions have either been characterized as a minimum heat input or as a critical mass-loss rate.

Emberley *et al.* have done extensive work focused on studying the self-extinguishment capabilities of one of the most commonly-used engineering timber products, namely Cross-laminated Timber (CLT), across different scales. In a bench-scale experimental study, different timber species and products were tested in a vertically-oriented Mass-loss Calorimeter (MLC). For all specimens, self-extinction occurred when the mass-loss rate decreased below 4.0 g/m^2s, regardless

of the heating history [10]. This result is consistent with values reported by other authors for the threshold condition to sustain the burning of wood cribs [11]. In a following bench-scale study [6], it is reported that the critical mass-loss rate for the self-extinction of six different types of timber ranged from 2.7 to 8.3 g/m^{2}s, while the corresponding critical external incident heat fluxes ranged from 24 to 57 kW/m^2 depending on the species. Later on, a large-scale test conducted using a compartment of Radiata Pine CLT with only two exposed timber surfaces [12] yielded that self-extinction was achieved when the incident heat flux over these surfaces decreased below 45 kW/m^2.

Bartlett *et al.* explored the occurrence of self-extinction of CLT through Rasbash's fire-point theory [13]. From an experimental study conducted testing horizontally-oriented bench-scale samples of CLT in a Fire Propagation Apparatus (FPA), the critical mass-loss rate for self-extinction was evaluated to be 3.5 g/m^{2}s , with a corresponding critical incident heat flux of 31 kW/m^2 [7].

In later work, three large-scale experiments were conducted using compartments with two exposed timber surfaces. Self-extinction failed in two of the tests due to the progressive delamination of the exposed timber walls. However, when self-extinction occurred, the critical mass-loss rate agreed with the bench-scale outcomes [14].

Crielaard *et al.* [8] defined self-extinction as the complete cease of combustion (both flaming and smoldering) and investigated its occurrence experimentally across scales; firstly, exposing horizontally-oriented CLT samples to incident heat fluxes of up to 75 kW/m^2 in a Cone Calorimeter, and secondly using medium-scale compartments (0.5x0.5 m^2 walls) were the timber surfaces were exposed to a constant 41 kW/m^2 incident heat flux, followed by a decay-phase type exposure. From these studies, it was concluded that CLT will self-extinguish if the external heat flux over the burning surfaces decreases below 5 to 6 kW/m^2. These values corresponded to the extinction of all smoldering reactions.

Cuevas *et al.* followed Bartlett *et al.*'s studies by conducting a bench-scale experimental study using FM Global's Fire Propagation Apparatus (FPA) to determine the conditions that lead to the self-extinction of horizontally-oriented CLT samples. This study better characterized the heat input and performed the tests under different oxygen concentrations in the surrounding atmosphere. It was found that timber self-extinguished when the mass-loss rate of the samples decreased below critical values of 3.4±0.4, 3.7±0.6, and 3.8±0.6 g/m^{2}s, when tested under atmospheres featuring 21%, 19%, and 17% oxygen content in volume, respectively [9]. The discrepancy in the results obtained from these studies is caused by the variability in species, experimental set-ups, and degree of control of the boundary conditions [15].

An additional limitation of existing studies is the exclusive focus on the solid-phase processes concerning the occurrence of self-extinction. Though this approach has undoubtedly provided understanding on how the self-extinction of timber occurs, it is not sufficient to fully explain or predict its occurrence accurately.

To overcome this issue, it is proposed that the analysis specific to the self-extinction of timber should be considered in the broader context of diffusion flame extinction [16–18]. For this purpose, it is possible to take advantage of the fact that despite the variety of experimental set-ups used, the totality of the bench-scale studies that have been conducted present scenarios that can be related to two canonical flame configurations; the boundary layer and the counter-flow diffusion flames. Within the context of this work, the latter is considered.

Setting the gas-phase problem in a context of counter-flow diffusion flames, Fendell [16] described the theoretical framework which can be extended to capture flame extinction over condensed fuels due to finite rate kinetics. By proposing an asymptotic analysis based on the expansion of the inverse of the first Damköhler number, this approach successfully describes the structure of the flame and the distribution of its bulk quantities.

The work was extended by Liñan [19], observing that the original description fell short of predicting the conditions for ignition and extinction. Focusing on the details of the gas phase near the stagnation plane and ignoring any consideration related to the condensed phase, Liñan conducted an asymptotic analysis expanding the ratio of the activation temperature to the characteristic temperature of the system. This allowed to describe the evolution of the flame structure for a wide range of Damköhler numbers and provided a clear description of the critical values at ignition and extinction. Nevertheless, this theoretical framework assumes fuel and oxidizer streams originating from an infinite source, so the solid properties which, in the present context, are responsible for timber self-extinction cannot be captured.

To characterize the impact of a condensed phase, Chao and Law [20] considered a stream of fuel originating from a condensed surface. The associated vaporization process affects the boundary conditions on the fuel side and therefore impacts the temperature field. The effect of radiative losses at the fuel surface was included to successfully capture their influence on the value of the Damköhler number.

Despite the significant advances introduced in this last formulation, a more detailed analysis of the solid phase is necessary to include the additional aspects associated with the combustion of a charring solid material. This more detailed treatment of the solid phase is needed to capture and understand the complete range of phenomena relative to the self-extinction of timber.

The work presented here is structured as follows; firstly, a theoretical framework based on the asymptotic analysis and study of the near-extinction conditions of a counter-flow diffusion flame established above the surface of a burning charring material will be presented. Following, the results derived from this model will be used to characterize the flame structure and to determine the conditions under which flame extinction is reached. Finally, the results obtained from the theoretical analysis will be combined with earlier experimental data obtained by Cuevas *et al.* with timber as solid fuel [9].

2 Theoretical framework

The following section presents the main equations governing the counter-flow flame analysis, which have been detailed for the most part in the works of Chao and Law [20], Liñan [19], and Fendell [16].

2.1 Governing equations

In the present configuration, the simultaneous mixing and reaction of opposing fuel and oxidizer streams occur in the vicinity of the stagnation plane, as shown in Figure 1.

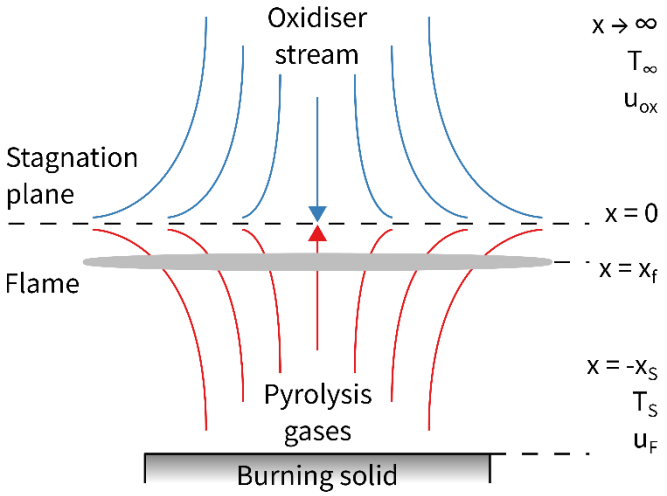

Figure 1: Schematics of the counter-flow diffusion flame over a solid fuel.

The fuel stream corresponds to pyrolysis gases that diffuse out of a semi-infinite slab of burning timber. It is assumed that the burning solid has a known surface temperature T_s and the rate of combustion is treated as a one-step irreversible first-order Arrhenius reaction. For simplicity, constant thermal properties and transport coefficients at the gas phase are assumed, along with a Lewis number equal to one [19]. In addition, since the characteristic time scales associated with the gas-phase processes are orders of magnitude smaller than those associated with the solid-phase [21], it is considered that the gas-phase adapts instantly to changes in the solid. To highlight the influence of the solid surface over the burning behavior and extinction of the flame, only radiative losses from the surface will be considered while gas-phase radiation will be ignored. The reader is invited to review the work

of Sohrab *et al.* [22] and the subsequent work of Chao *et al.* [23], where flame extinction was analyzed considering radiative heat losses from the flame. In both studies, the focus was on the gas phase, so solid-surface radiation was not considered.

Under these assumptions, the following equations describe the conservation of energy and species in the gas phase [16].

$$\tilde{x}\frac{d\tilde{T}}{d\tilde{x}} + \frac{d^2\tilde{T}}{d\tilde{x}^2} = -Da\tilde{Y}_F\tilde{Y}_{ox}exp\left(-\tilde{T}_a/\tilde{T}\right) \tag{1}$$

$$\tilde{x}\frac{d}{d\tilde{x}}\left(\tilde{T} + \tilde{Y}_l\right) + D\frac{d^2}{d\tilde{x}^2}\left(\tilde{T} + \tilde{Y}_l\right) = 0 \tag{2}$$

Where the following non-dimensionalizations were used,

$$Da = \nu_0 B\rho/(kW_F)$$

$$\tilde{T}_a = Ec_p/(Rq_c)$$

$$\tilde{T} = T/\left(q_c/c_p\right)$$

$$\tilde{Y}_i = Y_i/(\nu_i W_i/\nu_F W_F)$$

$$\tilde{q}_v = q_v/q_c$$

$$\tilde{x} = x\sqrt{k/D}$$

Where Da is the first Damköhler number, $\tilde{T}_a$ is the non-dimensional activation temperature, E is the activation energy of the reaction, R is the universal gas constant, ρ, and c_p are the local gas density and heat capacity, q_c and q_v are the heat of combustion and pyrolysis per unit mass of fuel, D is the mass diffusion coefficient, $\dot{\omega}_F'''$ is the reaction rate per unit mass of fuel, ν_i and W_i are the stoichiometric coefficient and molecular weight of the species i, x is the space coordinate in the direction normal to the fuel surface, and k is the strain rate of the fuel flow.

At the oxidizer side ($\tilde{x} \to \infty$), the boundary condition is defined by the following non-dimensional relations.

$$\tilde{T} \to \tilde{T}_{\infty} \tag{3}$$

$$\tilde{Y}_F \to 0 \tag{4}$$

$$\tilde{Y}_{ox} \to \tilde{Y}_{ox,\infty} \tag{5}$$

While at the surface of the burning solid, the following boundary conditions are imposed,

$$\tilde{T} = \tilde{T}_s \tag{6}$$

$$\frac{d\tilde{Y}_F}{d\tilde{x}} = \tilde{x}_s\left(\tilde{Y}_{F,s} - 1\right) \tag{7}$$

$$\frac{d\tilde{Y}_{ox}}{d\tilde{x}} = \tilde{x}_s\tilde{Y}_{ox,s} \tag{8}$$

In the last two expressions, $\tilde{x}_s$ represents the non-dimensional stand-off distance of the stagnation plane, which is directly related to the burning rate of the fuel through the following relation [20],

$$k = \dot{m}_F''/(\rho x_s) \tag{9}$$

Where ρ is the density of the pyrolysis gases, and $\dot{m}_F''$ is the flow of pyrolysis gases (fuel) leaving the solid per unit area, assumed to be constant over the solid surface.

The final boundary condition is provided by the heat exchange taking place at the pyrolysis front. As illustrated in Figure 2, a control volume is introduced for the char region, and a comprehensive energy balance (Eq.(10)) enables the definition of the net energy available for fuel generation.

$$\dot{q}_f'' + \dot{q}_{ext}'' + \dot{q}_{ch}'' = \dot{m}_p'' q_v + \dot{q}_{loss}'' + \dot{q}_{in}'' + \frac{d\delta\dot{q}_{st}''}{dt} \tag{10}$$

The terms on the left-hand side represent the heat provided to the solid by the flame $\dot{q}_f''$, an external heat flux $\dot{q}_{ext}''$, and the superficial char oxidation reaction $\dot{q}_{ch}''$. These terms must balance the energy required to generate pyrolysis gases $\dot{m}_p'' q_v$, the re-radiation heat losses at the surface $\dot{q}_{loss}''$, the heat that is conducted into the material past the pyrolysis front $\dot{q}_{in}''$, and the increase in energy stored within the char layer (control volume) $d\delta\dot{q}_{st}''/dt$. Based on the analysis of Emberley *et al.* [10], this last

term can be neglected as a thermal steady-state is reached within the char early in the burning process. Following, the energy balance can be rearranged and expressed as follows

$$\lambda \frac{\partial T}{\partial x} = \dot{m}_p'' q_v + \left(1 + \frac{\dot{q}_{in}''}{\dot{q}_{loss}''} - \frac{\dot{q}_{ext}''}{\dot{q}_{loss}''} - \frac{\dot{q}_{ch}''}{\dot{q}_{loss}''}\right) \cdot \dot{q}_{loss}''$$

$$\Longrightarrow \lambda \frac{\partial T}{\partial x} = k\rho x_s q_v + \Omega \cdot \dot{q}_{loss}'' \tag{11}$$

Where the heat provided by the flame has been expressed as a conductive heat flux through the gas-phase conductivity λ, and the term Ω is defined as

$$\Omega = -\frac{\dot{q}_{ext}''}{\dot{q}_{loss}''} + \left(1 + \frac{\dot{q}_{in}''}{\dot{q}_{loss}''} - \frac{\dot{q}_{ch}''}{\dot{q}_{loss}''}\right) \tag{12}$$

And embodies the overall heat balance at the pyrolysis front, normalized by the radiative heat losses at the surface. It is important to notice that the variations in the participating heat fluxes are happening at time scales orders of magnitudes larger than the processes driving flame extinction. Consequently, they can be treated as constant values defined by the conditions studied, enabling the inclusion of Ω in a way that incorporates the role of the char but maintaining consistency with previous work [20].

Furthermore, in Eq.(11) the mass flow of pyrolysis gases has been expressed in terms of the gases density, strain rate, and the relative distance between the stagnation plane and the surface of the solid x_s. By introducing the non-dimensional variables previously described, Eq.(11) is then expressed as

$$\frac{\partial \tilde{T}}{\partial \tilde{x}} = \tilde{x}_s \tilde{q}_v + \frac{\Omega \mu \sigma}{(\rho c_p k \lambda)^{1/2}} \left(\frac{q_c}{c_p}\right)^3 \left(\tilde{T}_s^4 - \tilde{T}_\infty^4\right) \tag{13}$$

where $\tilde{q}_v$ is the non-dimensional effective heat of pyrolysis. Furthermore, the second term on the right-hand side can be reduced by introducing a new parameter that describes the ratio between the net heat balance at the surface to the heat diffused from the flame, R_a [20], defined as

$$R_a = \frac{\Omega\mu\sigma}{(\rho c_p k\lambda)^{1/2}}\left(\frac{q_c}{c_p}\right)^3 \tag{14}$$

R_a is a function of the strain rate and therefore amalgamates the full coupling of the solid and gas phases. Finally, rewriting Eq.(13) in terms of R_a delivers,

$$\frac{d\tilde{T}}{d\tilde{x}} = \tilde{x}_s\tilde{q}_v + R_a\left(\tilde{T}_s^4 - \tilde{T}_\infty^4\right) = \tilde{x}_s\tilde{q}_v + R_T \tag{15}$$

It is important to notice that due to the inclusion of Ω, the previous expression consolidates all the participating heat fluxes within the control volume presented in Figure 2, thus delivering a boundary condition at the pyrolysis front, not at the solid surface as initially proposed by Chao and Law [20].

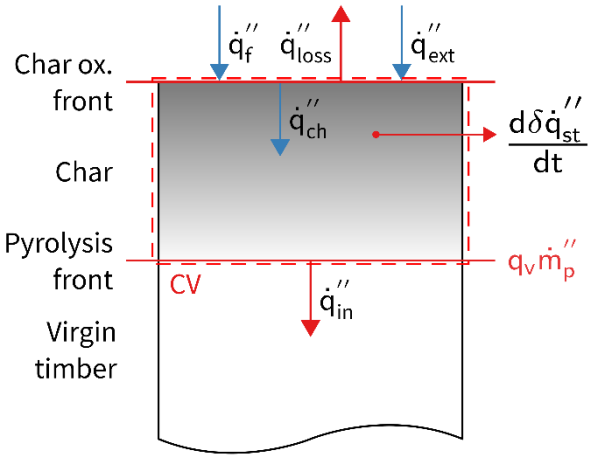

Figure 2: Schematics of the heat exchange taking place at the solid phase.

Through the inclusion of Ω in Eqs. (13) to (15), the system of equations that describe the state of the counter-flow flame is analogous to the one presented by Chao and Law [20] (Subsection 2.1 of [20]). Therefore, the same solving procedure can be applied (Subsection 2.2 of [20]). The reader is invited to review the original article for a detailed description of the solving procedure, as only the required equations and calculation steps will be reproduced here when necessary.

3 Results and Discussion

3.1 Model parameters

Based on the works of Roberts *et al.* [24] and Rasbash [25], formaldehyde (CH_2O) is used as a surrogate to the pyrolysis gases of timber. By treating combustion as a high-activation-energy process, the details of the chemistry are neglected and the use of formaldehyde as a fuel surrogate affects mainly the kinetic parameters and stoichiometric coefficients defined by the overall one-step reaction. The thermal properties of the fuel were taken from [26–28], while the kinetic parameters were extracted from [27,29].

Oxygen contents of 17%, 19%, and 21%, along with external incident heat fluxes ranging from 30 to 50 kW/m^2 were considered, to replicate the experimental conditions presented in Cuevas *et al.* [9]. In this study, the samples were initially subjected to an incident heat flux of 50 kW/m^2 until a thermal steady state is reached within the sample [10]. After this, the magnitude of the incident heat flux is decreased to a set value to determine the threshold conditions that allowed to sustain flaming combustion. The sample dimensions and preparation were designed to ensure one-dimensional heating and a semi-infinite-solid behavior throughout the experiment [15]. During the experiments, the evolution of the in-depth temperature and the mass of the sample were recorded. The time to self-extinction was recorded to retrieve the instantaneous mass-loss rate and thermal state of the sample, regression of the exposed surface, and the true external incident heat flux over it. For more details on the instrumentation and methodology used, the reader is invited to review the original article [9].

For the radiative exchange at the surface of the solid, an ambient temperature of 20°C is considered. Charred plywood is used as a surrogate for the surface emissivity of timber [30]. The heat provided by the char oxidation reaction is evaluated from the data presented by Emberley *et al.* [31] and the experimental results presented by Spearpoint *et al.* [32]. Following Emberley *et al.* [10], The amount of heat being

conducted into the material is estimated using the in-depth temperature measurements from the experiments presented in [9].

Surface temperature is approximated as the temperature registered by the embedded thermocouple closer to the heated surface until exposure occurred due to the continuous regression of the exposed surface. After this, T_s is taken as the last valid reading of the remaining embedded thermocouples before being exposed out of the burning sample. When a thermocouple becomes exposed, the smoothness of the data collected decreases. A rate of change of 25% of the nominal thermocouple uncertainty per second is defined as the threshold value to define the occurrence of thermocouple exposure. An example of this procedure is presented in Figure 3(a). After the exposure of the initial thermocouple, T_s was approximated as the last valid reading of the remaining thermocouples embedded in the solid. Figure 3(b) shows the estimated surface temperature for the complete set of repetitions conducted for a given set of oxygen content and external incident heat flux. Finally, as discussed by Cuevas *et al.* [9], when flame extinction occurred, it happened almost instantaneously after the reduction in the magnitude of the external incident heat flux. Based on the assumption that the characteristic time-scales of solid-phase processes are longer than the ones in the gas-phase, the surface temperature was considered to vary solely with the oxygen content, and values of 600, 625, and 650°C were evaluated from the experiments conducted at oxygen contents of 17%,19%, and 21% respectively.

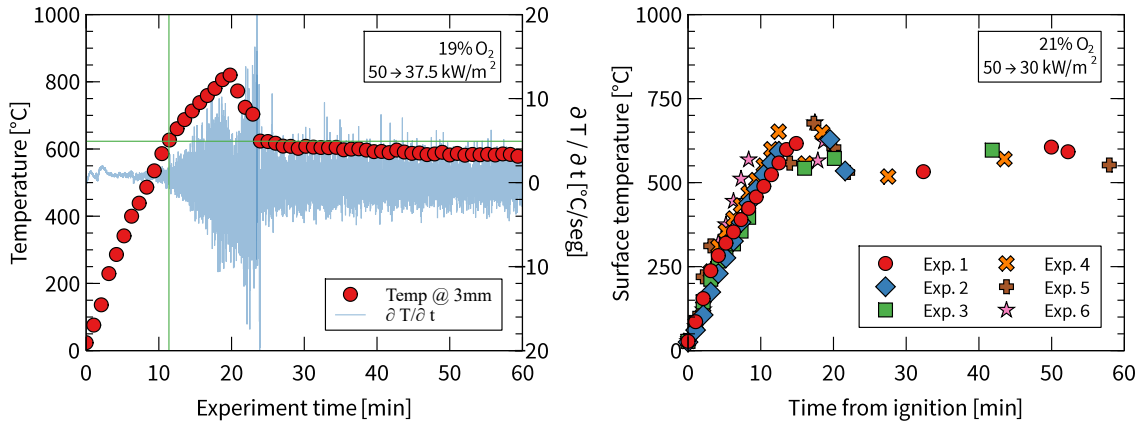

(a) *(b)*

Figure 3: Surface temperature approximation. (a) Detection of thermocouple exposure. (b) Approximated surface temperature for a given experimental condition.

3.2 Energy balance at the solid

Based on the approach just presented to quantify the participating heat fluxes present in Eq.(12), it can be seen that $\dot{q}''_{loss}$, $\dot{q}''_{in}$, and $\dot{q}''_{ch}$ are defined ultimately as functions of $\dot{q}''_{ext}$. Consequently, Ω can be described and evaluated as a function of only two independent variables, namely $Y_{ox,\infty}$ and $\dot{q}''_{ext}$, as illustrated in Figure 4.

The effect of $\dot{q}''_{ext}$ over Ω is multiple. Increasing the magnitude of $\dot{q}''_{ext}$ increases the energy accumulated at the surface, raising its temperature and therefore the magnitude of surface radiative losses $\dot{q}''_{loss}$, but also the intensity of solid combustion processes $\dot{q}''_{ch}$ and, in turn, the amount of heat conducted inwards, $\dot{q}''_{in}$. Over the range of external heat fluxes considered, $\dot{q}''_{loss}$, $\dot{q}''_{ch}$, and $\dot{q}''_{in}$ are generally orders of magnitude smaller than $\dot{q}''_{ext}$, and their specific contribution to the evaluation of Ω is limited to the magnitude of $\dot{q}''_{ext}$. In general terms, for a fixed oxygen content, Ω is found to decrease linearly when increasing the magnitude of $\dot{q}''_{ext}$.

In addition, for a fixed external incident heat flux, Ω increases when the oxygen content decreases. Phenomenologically, this behavior is attributed to the reduction in the rate of the char oxidation reaction taking place at the solid's surface ($\dot{q}''_{ch}$) that also lowers the rate of regression of the exposed surface, increasing the thickness of the char layer, and consequently reducing the amount of heat conducted inwards ($\dot{q}''_{in}$).

It is crucial to notice that, for lower magnitudes of $\dot{q}''_{ext}$, Ω is positively-valued, meaning that that the second term of Eq.(12) out weights the first one. This indicates that the detrimental effects of $\dot{q}''_{in}$ and $\dot{q}''_{loss}$ dominate over $\dot{q}''_{ext}$ and $\dot{q}''_{ch}$. As a consequence, Ω represents the heat being dissipated by the burning solid. As $\dot{q}''_{ext}$ increases, a critical point is reached when Ω (and consequently R_a) equals zero, indicating that adiabatic conditions are met at the surface of the solid. Furthermore, this pivotal condition signifies a fundamental change of the regime taking place at the solid surface; if $\dot{q}''_{ext}$ is further increased, the overall heat losses at the surface are surpassed, and therefore Ω denotes the heat gained by the burning solid.

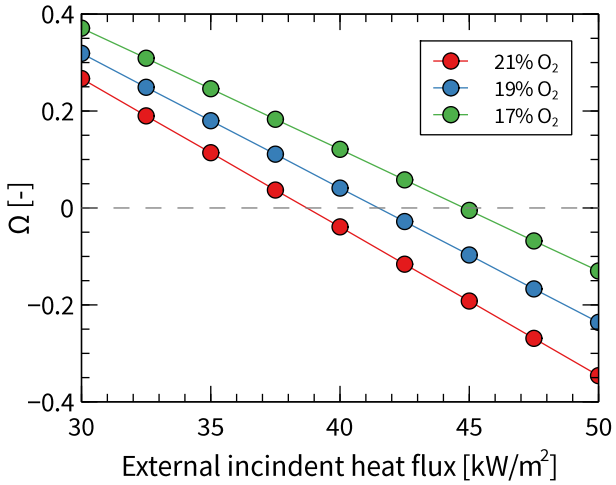

Figure 4: Variation of Ω as a function of the external incident heat flux and oxygen content.

3.3 Bulk flame properties

The non-dimensional position of the solid surface relative to the stagnation plane $\tilde{x}_s$ is approximated by Chao and Law [20] as

$$\tilde{x}_s = \tilde{x}_{s,0} - \varepsilon\phi\tilde{x}_{s,1} + O(\varepsilon^2) \tag{16}$$

Where $\tilde{x}_{s,0}$ is the unperturbed solution, and $\varepsilon\phi\tilde{x}_{s,1}$ is the amplitude of the perturbation about $\tilde{x}_{s,0}$, where the expansion parameter ε is evaluated in terms of the non-dimensional flame temperature as $\varepsilon = \tilde{T}_f^2/\tilde{T}_a$. The value of $\tilde{x}_{s,0}$ can be evaluated from the following expression derived by Chao and Law,

$$\left(\sqrt{\pi/2} + I\left(\tilde{x}_{s,0}\right)\right)\left(\tilde{x}_{s,0}\tilde{q}_v + R_T\right)exp\left(\tilde{x}_{s,0}^2/2\right) = \tilde{Y}_{o,\infty} - \left(\tilde{T}_s - \tilde{T}_\infty\right) \tag{17}$$

Where $I(\tilde{x}) = \int_0^{\tilde{x}} exp(-t^2/2)dt$ is defined as an auxiliary function.

Furthermore, the flame temperature and position relative to the stagnation plane are obtained from the following expressions

$$\tilde{T}_f \approx \tilde{T}_\infty + \frac{\tilde{Y}_{ox,\infty}}{1+\tilde{Y}_{ox,\infty}}\left(1 + \left(\tilde{T}_s - \tilde{T}_\infty\right) - \tilde{q}_v - \frac{R_T}{\tilde{x}_{s,0}}\right) \tag{18}$$

$$I\left(\tilde{x}_f\right) \approx \sqrt{\pi/2} - \frac{\tilde{Y}_{ox,\infty}}{1+\tilde{Y}_{ox,\infty}}\left[\left(\sqrt{\pi/2} + I\left(\tilde{x}_{s,0}\right)\right) + exp\left(-{\tilde{x}_{s,0}}^2/2\right)/\tilde{x}_{s,0}\right] \tag{19}$$

The behavior of the flame bulk properties as a function of $\dot{q}''_{ext}$ and oxygen content is presented in Figure 5(a) and plotted against the parameter R_a. The interpretation of the results presented herein should be made with care since R_a is not an independent variable in the problem. Each plotted point thus corresponds to a potential solution of the set of equations previously described, which the corresponding physical system may adopt as combustion occurs. Nevertheless, the general trends and features shown can still be described in terms of physical phenomena as ranges of possible values are quantified. The analysis of the results has been broken down as follows

3.3.1 Heat-losses regime

When the overall heat balance at the control volume defined in Figure 2 yields that heat is being lost, positive values of Ω lead to positive values of R_a, as shown by Eq.(11). The range of external incident heat fluxes that leads to a heat-loss scenario also varies as a function of the oxygen content considered, as seen in Figure 4. Virtually increasing the re-radiation losses at the surface by increasing the magnitude of R_a, will reduce flame temperature as more of the energy generated in the gas-phase needs to be diverted towards the solid, where a decrease in the rate of fuel vaporization will also be experienced. This behavior is observed in Figure 5(b), regardless of the oxygen concentration.

The reduction in flame temperature and the increase in the rate of heat being lost will decrease the fuel gasification rate for a given oxygen concentration. Consequently, the dynamic pressure of the fuel stream diffusing out of the solid will

decrease, pushing the stagnation plane closer to the solid surface until the pressure equalizes at both sides of the plane [33], as shown in Figure 5(c). As indicated by Chao and Law [20], $\tilde{x}_{s,0}$ decreases linearly due to its direct relation to the difference between the energy transferred and the energy lost at the surface of the solid, as described by Eq.(15).

To analyze the behavior shown by $\tilde{x}_f$, it is necessary to highlight the fact that the counter-flow flame will be established in the region where near-stoichiometric conditions are met. As described by Turns [33], most hydrocarbon fuels burning in air require substantially more air than fuel to reach stoichiometric conditions. Under this scenario, fuel must diffuse through the stagnation plane towards the flame, located at the oxidizer side. A decrease in the fuel gasification rate means that less fuel diffuses through the stagnation plane, and consequently, stoichiometric conditions are met closer to it. Consequently, increasing Ra will cause a decrease of $\tilde{x}_f$ regardless of the oxygen concentration, as shown in Figure 5(d).

As the heat losses tend to zero ($R_a \to 0$), adiabatic conditions are attained at the pyrolysis front. On the other hand, as the magnitude of the heat losses at the surface increases, the flame bulk properties decrease towards minimum values ($\tilde{x}_{s,0}^{min}$, $\tilde{x}_f^{min}$, $\tilde{T}_f^{min}$) that represent the point after which the flame structure equations stop having a solution. Physically, the reduction of flame temperature has pushed the system to a point where reaction kinetics are slow enough to trigger the extinction of the flame. Thus, for a given external incident heat flux, the system admits a defined range of heat losses in which a flame can be sustained.

Furthermore, as the magnitude of the external incident heat flux increases, less energy generated in the combustion reaction needs to be diverted to the solid to produce the vaporization of fuel, allowing the combustion process to be sustained at lower energetic levels in both the solid phase and the gas phase. Consequently, the magnitude of $\tilde{T}_f^{min}$ and $\tilde{x}_{s,0}^{min}$ both decrease when increasing $\dot{q}''_{ext}$, regardless of the oxygen content. Finally, a decrease in the minimum allowable fuel gasification rate

will also shift the minimum relative position of the flame towards the stagnation plane $\tilde{x}_f^{min}$, based on the arguments previously presented. Thus, increasing $\dot{q}''_{ext}$ expands the range of heat losses under which the flame can be sustained.

3.3.2 Heat-gains regime

If the external heat flux is increased enough, the energy balance at the char layer becomes favorable as heat is gained, yielding negative values of Ω and Ra.

An increase in the rate of heat being gained will be translated into an increased pyrolysis rate, enhancing the flow of fuel diffusing out of the solid. As a consequence, the stand-off distance of the stagnation plane will grow. The increase in the flow of fuel towards the stagnation plane will also raise the amount of fuel that diffuses through it, displacing the stoichiometric-mixture region and therefore increasing $\tilde{x}_f$. Finally, because of the increased amount of fuel being supplied, the flame temperature will also rise.

In this regime ($R_a \leq 0$), the minimum values of the flame bulk properties correspond to the previously described scenario where adiabatic conditions are met at the surface of the solid. As the rate of heat gained at the pyrolysis front increases ($R_a \to -\infty$), the fuel gasification rate will virtually grow unbounded, pushing the stagnation plane away from the fuel surface. On the other hand, the flame temperature and position relative to the stagnation plane will converge to asymptotic values as the flame approaches its adiabatic state.

In this regime, despite the increase in strain rate (due to the surge in fuel velocity), the contribution of $\dot{q}''_{ext}$ to the system is enough to sustain infinitely-fast kinetics at the gas phase. Thus, regardless of the residence time of the fuel gases within the flame (modified by the strain rate), flame extinction by blow-off is never achieved.

3.3.3 Influence of oxygen content

Decreasing the oxygen content will negatively affect gas-phase reactivity, as shown in Eq.(1). Consequently, for a given magnitude of R_a and $\dot{q}''_{ext}$, flame temperature

will decrease when reducing the oxygen content, regardless of the scenario at the surface of the solid (heat gained or lost).

As the flame temperature is reduced, less energy is provided from the flame towards the solid fuel. As a consequence, the stand-off distance of the stagnation plane will decrease with the oxygen content. This process can be linked to the linear relation described by Eq.(15), where a reduction in the flame temperature due to a depletion in the oxygen content will decrease the gas-phase temperature and correspondingly the thermal gradient at the solid-gas interphase. Thus, for a given heat exchange at the surface (R_T), $\tilde{x}_s$ (and consequently $\tilde{x}_{s,0}$) will decrease. Even though the functional relations are more complex, the same trend is obtained when inspecting Eq.(17), where it can be seen that a reduction in the right-hand side of the equation must be compensated by a decrease in the magnitude of $\tilde{x}_{s,0}$, for a given magnitude of R_T (and of course set $\tilde{q}_v$).

In the regime where heat is gained ($\Omega < 0$), a decrease in the oxygen content means that less fuel is necessary to achieve the stoichiometric-mixture condition at the flame. For a given flow of fuel diffusing through the stagnation plane, this means that the fuel will have to diffuse further in order to achieve the required concentration. As a consequence, flame location $\tilde{x}_s$ will increase when reducing the oxygen content. It is important to remember that the maximum values within this regime also correspond to the adiabatic-flame scenario, and therefore their behavior will be identical to the one reported for $\tilde{T}_f$. When heat is lost at the surface, the curves exhibit a change of slope when increasing R_a. As already mentioned, an increase in the heat losses at the surface will decrease flame temperature and the pyrolysis rate, weakening the flame. Thus, an additional detrimental effect like oxygen depletion will reduce the solution space where the flame can be established even further. Ultimately, the lower the oxygen content, the faster the flame position will tend towards its minimum value.

If, for a given $\dot{q}''_{ext}$, the minimum values reached by the flame bulk properties within the heat-loss regime increase when decreasing the oxygen content, then variations in the oxygen content modify the range of external incident heat fluxes where a

heat-loss scenario at the char layer is found. This is illustrated by the behavior shown by $\tilde{T}_f$ (Figure 5(b)), $\tilde{x}_{s,0}$ (Figure 5(c)), and $\tilde{x}_f$ (Figure 5(d)), under an external heat flux of 40 kW/m^2: under a 17% or 19% oxygen content, there is an overall negative heat balance at the char layer, while this external heat flux corresponds to a positive heat balance under a 21% oxygen content. The contribution of the external incident heat flux at 17% and 19% oxygen content provides enough energy to compensate for the reduction in reaction rate caused by decreasing the oxygen content. Consequently, lower values of $\tilde{x}_{s,0}^{min}$, $\tilde{x}_f^{min}$, $\tilde{T}_f^{min}$ are obtained when compared to the minimum values found at higher oxygen contents.

So far, the expressions that describe the evolution of $\tilde{x}_{s,0}$, $\tilde{x}_f$, and $\tilde{T}_f$ are derived assuming infinitely-fast chemistry. To investigate flame extinction, high-activation-energy asymptotics are used [34]. Under this framework, the gas phase is composed by an $O(\varepsilon)$ −thick reactive region around the area of maximum temperature, surrounded by two non-reactive regions, where the chemical reaction is frozen due to the reduced temperature [19]. The equations that describe the structure of these reactive and non-reactive regions, described extensively in the work of Chao and Law [20], were evaluated numerically. The results of this process are presented in the following section.

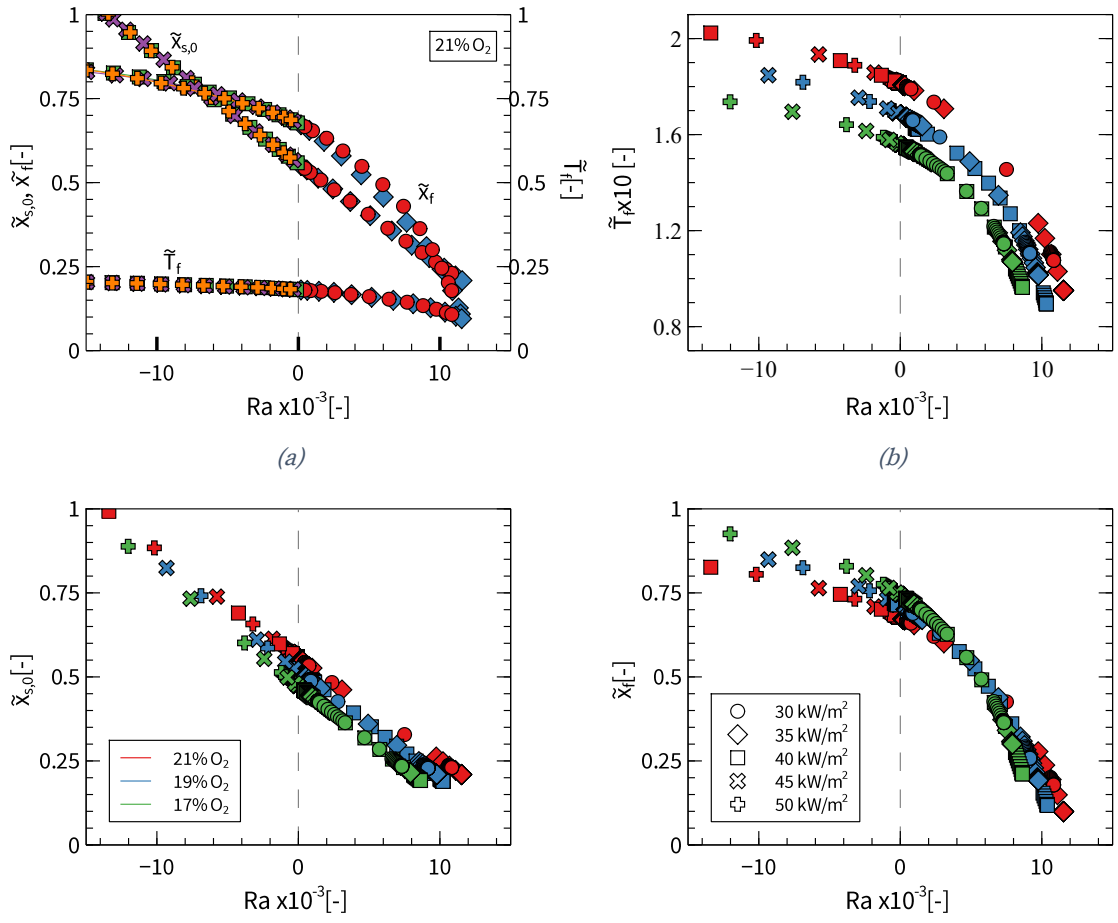

Figure 5: Evolution of the normalized stagnation flame bulk properties as a function of R_a for different oxygen contents and external incident heat fluxes.

3.4 Flame extinction

Near extinction, the flame temperature decreases, its reaction rate declines, and reactant leakage through the reaction front increases. As shown by Chao and Law. [20], reactant leakage is captured through the expansion constant a_1, defined in Eq.(20), that accounts for the reduction in temperature due to this effect. Therefore, the evolution of this surrogate quantity can be used to determine the conditions under which extinction occurs [35].

$$\tilde{T}^{+} \approx \tilde{T}_{\infty} + \left[a_0 - \varepsilon\left(\tilde{T}_f^{*}/\tilde{T}_f\right)^2\left(a_1/\tilde{Y}_{ox,\infty}\right) + O(\varepsilon^2)\right]\left(\sqrt{\pi/2} - I(\tilde{x})\right) \tag{20}$$

In this expression, $\tilde{T}_f^{*}$ corresponds to the non-dimensional adiabatic flame temperature. Figure 6 presents the evaluation of a_1 as a function of Da for a range of external incident heat fluxes and oxygen contents. Physically, an increase in a_1

indicates a decrease in the flame temperature, meaning that the flame tends towards extinction. Although two values of a_1 provide a mathematical solution to the problem, only the lower branch has an actual physical meaning and is presented hereafter [19,20]. There, a_1 increases as Da decreases up to a critical value after which the canonical system of equations does not yield a solution. This decrease in Da can be translated into an increase in the velocity of the reactants, which reduces the fuel residence time. If the residence time becomes smaller than the characteristic time of the combustion reaction, extinction will occur. Thus, a critical Damköhler number denoting extinction by flame blow-off is identified. This extinction mechanism is found for all of the external incident heat fluxes and oxygen contents studied.

Depending on the magnitude of Ω, two different behaviors of a_1 are identified for increasing values of Da. For positive values of Ω, and consequently a negative heat balance at the char layer, a_1 increases rapidly when approaching an upper-bound value of Da, which depends on the oxygen content and external incident heat flux studied. Beyond this critical value, the canonical system of equations does not yield a solution, meaning that a flame cannot be established. All other parameters being set, an increasing Damköhler number can be translated into a decreasing strain rate, and due to the definition of the strain rate presented in Eq.(9), this ultimately denotes a declining flow of fuel. If the fuel supply drops below a critical value, the energy generated by the combustion reaction cannot overcome the heat losses, the flame temperature decreases, and the flame tends to extinction. Thus, the upper bound found in this regime for the Damköhler number denotes flame extinction by quenching. For negative values of Ω, and consequently a positive heat balance at the char layer, the reduction in flame temperature decreases asymptotically towards zero when the Damköhler number goes to infinity. Flame extinction by quenching is consequently not reported in this regime.

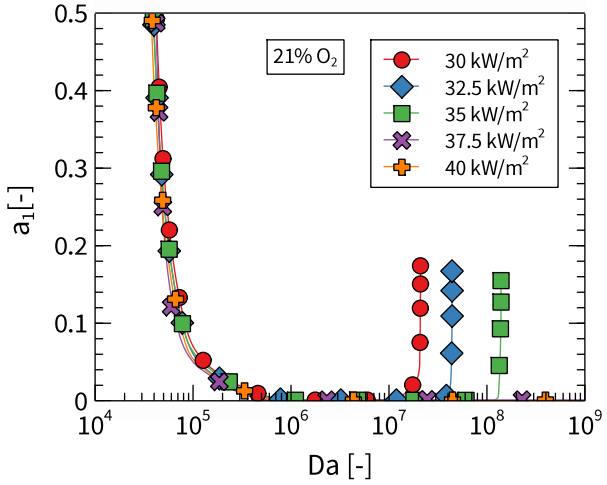

Figure 6: Variation of the flame reactant leakage parameter a_1, as a function Da, for different external incident heat fluxes at 21% oxygen content.

The evolution of the critical Damköhler numbers at extinction by quenching $Da_{c,q}$ and blow-off $Da_{c,b}$ as a function of $\dot{q}''_{ext}$ and the oxygen content is presented in Figure 7(a) and (b), respectively. For a given $\dot{q}''_{ext}$, $Da_{c,b}$ increases with decreasing oxygen content and the domain of flame existence is thus reduced. Since, as illustrated in Eq.(1), the oxygen content has a direct impact on the reaction rate and a secondary influence through the pre-exponential factor B, a reduction in oxygen content weakens the reaction and further facilitates extinction by blow-off. For a fixed oxygen content, the small impact of $\dot{q}''_{ext}$ on $Da_{c,b}$ is caused by a balance between two mechanisms: on the one hand, the increase in external heat flux supports fuel production in the solid phase, but it simultaneously increases the velocity of the fuel stream, consequently lowering the residence time. Overall, the domain where the flame can be sustained is marginally affected.

Regarding the occurrence of flame extinction by quenching, decreasing the oxygen content for a fixed external incident heat flux decreased $Da_{c,q}$. Decreasing the oxygen content will result in a weaker flame, meaning that more fuel needs to be provided to sustain the combustion process. As a result, away from the blow-off limit, the magnitude of the minimum fuel velocity required to sustain the flame is increased, therefore decreasing the value of $Da_{c,q}$.

On the other hand, it was found that increasing $\dot{q}''_{ext}$ increases $Da_{c,q}$. This is because the flame needs to provide less energy to compensate for the heat losses at the burning solid. This reduced heat sink allows for weaker flames to be sustained at lower fuel velocities, increasing ultimately the value of Da_q.

It is interesting to notice how Da_q tends to infinity for negative Ω values. As previously discussed, extinction by quenching is not captured in this regime.

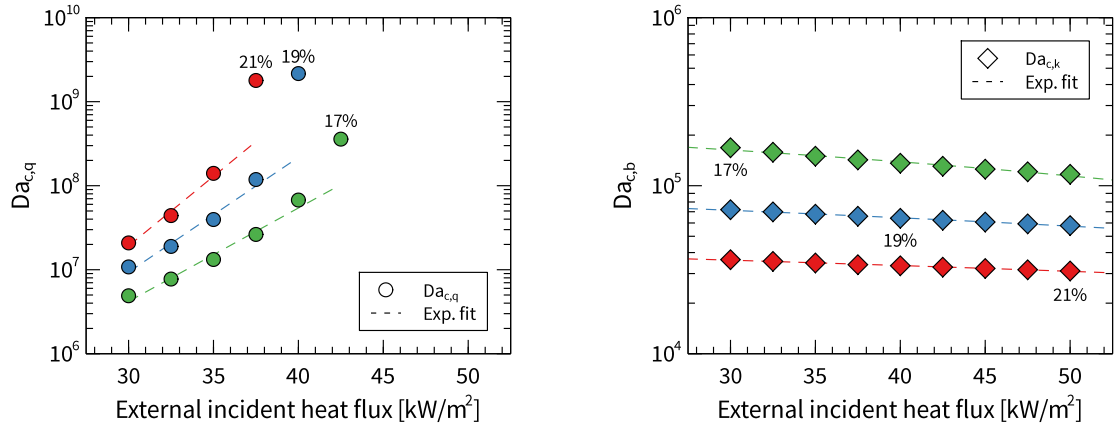

(a) *(b)*

Figure 7: Critical Damköhler numbers at extinction as a function of the external incident heat flux for the different oxygen contents studied. (a) Quenching extinction, (b) Blow-off extinction.

3.5 Benchmarking against experimental results

Results from this theoretical framework are contrasted against previously described experimental data by Cuevas *et al.* on flame extinction. Though flame extinction is a transient phenomenon, it is assumed to be the immediate consequence of slower variations in the solid phase. As such, the gas-phase in these experiments is considered as a succession of pseudo-steady states to enable the comparison of experimental data with the theoretical Damköhler number at quenching. Furthermore, the experimental strain rate is evaluated as

$$k_{exp} = (\dot{m}''_F/\rho)/w \tag{21}$$

where $\dot{m}''_F$ is the experimental mass-loss rate per unit area of the test sample. The experimental Damköhler at quenching, $Da_{q,exp}$, follows the same trends predicted by the theoretical model, as illustrated in Figure 8. $Da_{q,exp}$ increases with both oxygen content and external incident heat flux. Nevertheless, $Da_{q,exp}$ is found to be

considerably less sensitive to the influence of these parameters when compared to the results from the theoretical model. Because of this lack of sensitivity, $Da_{q,exp}$ behaves as if it were practically insensitive to variations in $\dot{q}''_{ext}$, and with reduced sensitivity to variations in the oxygen content. Nonetheless, this behavior is consistent with the trends observed from the mass-loss rate at extinction presented in [9].

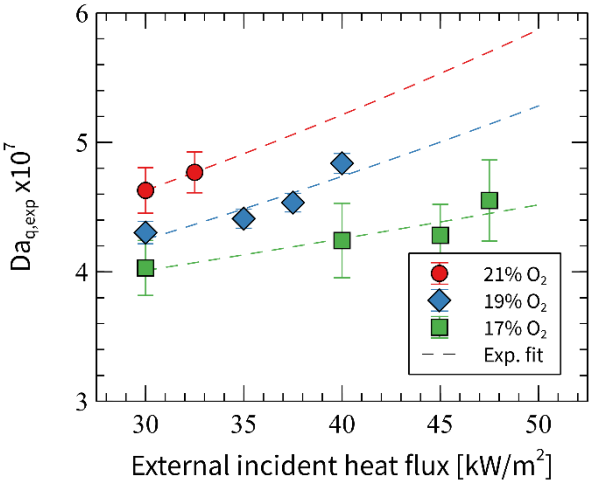

Figure 8: Experimental critical Damköhler number at quenching as a function of the different oxygen contents and external incident heat fluxes considered.

Figure 9 presents the ratio between the critical Damköhler number for extinction by quenching derived from the experimental results $Da_{q,exp}$, and the one derived from the theoretical model $Da_{q,theo}$. Good agreement between the experimental and theoretical results is found for values of $\dot{q}''_{ext}$ above 30 kW/m^2, indicating that the theoretical model is, in general terms, adequately capturing the effect of the most critical processes taking place in the experiments.

However, the theoretical model underestimates the critical Damköhler number at quenching, for an external incident heat flux of 30 kW/m^2 and all the oxygen contents considered. This is translated into an overestimation in the critical mass-loss rate for quenching at extinction compared to the experimental results. Furthermore, the level of overestimation increases as the oxygen content was decreased.

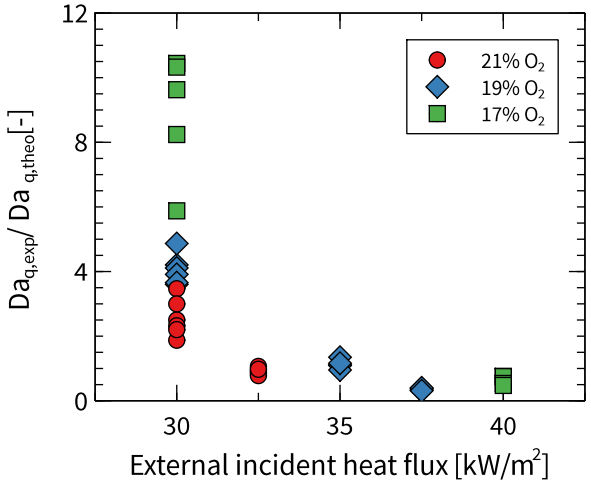

Figure 9: Ratio of the experimental to theoretical Da at quenching as a function of the external incident heat flux for the different oxygen contents studied.

It is proposed that missing phenomena, not incorporated into the theoretical model so far, are causing this mismatch between theoretical and experimental results. For example, the fuel diffusing out of the solid has been considered as pure, whereas in reality, the pyrolysis gases are a complex mixture of combustible gases, water vapor, and non-combustible compounds also generated during the thermal decomposition of timber [24]. Moreover, the solid-phase combustion reaction taking place at the exposed surface of the material (only considered now for its role in Ω) will consume a fraction of the combustible gases diffusing out of the solid and release non-combustible gaseous products [36,37]. Consequently, the actual amount of fuel that reaches the reaction zone of the flame will be only a fraction of the amount generated initially. In other words, fuel depletion will occur at the solid surface.

3.6 Depletion factor

The strength of the superficial combustion reaction is a function of the amount of oxygen available in the vicinity of the surface and the rate of heat being externally supplied to the surface of the burning timber element [38,39]. Therefore, this reaction (and consequently the depletion of fuel) is more intense when the oxygen content and $\dot{q}''_{ext}$ are higher.

To represent the depletion of fuel, it is considered that the combustible mixture leaving the solid (pyrolysis gases) is a combination of formaldehyde, as previously considered, and an inert diluent. In other words,

$$Y_P = Y_F + Y_I \Rightarrow Y_F = Y_P(1 - Y_I/Y_P) \tag{22}$$

Where Y_P, Y_F, and Y_I are the mass fractions of pyrolysis gases, pure fuel, and inert diluent, respectively. Following, the purity of the fuel Ψ is defined as

$$\Psi = (1 - Y_I/Y_P) \tag{23}$$

Then, Ψ will vary between zero ($Y_F = 0$) and 1 ($Y_I = 0$) depending on the amount of inert diluent considered. Thus,

$$Y_F = Y_P\Psi \equiv Y_F^* \tag{24}$$

And therefore, the following updated expression is obtained for the mass diffusion boundary condition taking place at the surface of the solid:

$$\rho D \frac{\partial Y_F^*}{\partial x} = \left(Y_{F,s}^* - 1\right)\dot{m}_{F,s}^{*\prime\prime} \tag{25}$$

It is essential to highlight that Ψ cannot be evaluated experimentally in the studied configuration, but it is calibrated for each oxygen content and external incident flux to account for the discrepancies between theoretical and experimental extinction Damköhler numbers. A reference dilution factor is adopted at an oxygen content of 17% and $\dot{q}''_{ext}$ equal to 30 kW/m^2 to study the evolution of Ψ as a function of the oxygen content and external radiative heat flux, as it is proposed that under these conditions fuel depletion will be at its weakest.

For a fixed oxygen content, Ψ decreases exponentially when increasing $\dot{q}''_{ext}$, meaning that the fuel is depleted as the external heat flux increases. As previously proposed, increasing $\dot{q}''_{ext}$ will provide more energy to the surface combustion reaction. This will cause a rise in the flow of inert gases being generated, increasing fuel dilution at the surface. In contrast, for a fixed value of $\dot{q}''_{ext}$, decreasing the oxygen content increases Ψ, so less fuel is swapped for inert diluent at the surface. This is caused by a reduction in the rate of surface combustion, leading therefore to

less inert products being added to the fuel mix. With this, the behavior of the fuel depletion process is found to agree with the expected behavior of the surface reaction described in Section 3.5.

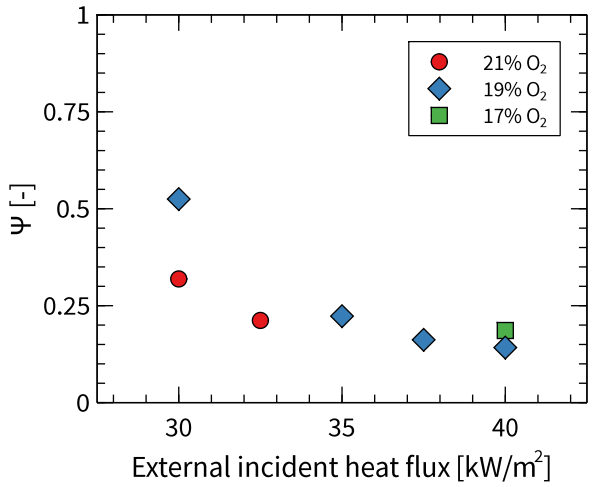

Figure 10: Purity of the pyrolysis gases Ψ as a function of the oxygen content and external incident heat flux applied.

4 Conclusions

In the present work, the self-extinction of timber is examined through the analysis of a counter-flow diffusion flame which considers heat transfer at the char layer through a heat exchange parameter Ω. For positive values of Ω, the pyrolysis front features a net heat loss. In this regime, bulk flame properties such as the stagnation plane stand-off distance, the flame position and temperature decrease with Ω. For negative values of Ω, the pyrolysis front gains heat through the exposed surface of the char layer. The stand-off distance of the stagnation plane grows unbounded for increasingly negative values of Ω, while the flame position and temperature increase asymptotically towards their adiabatic values.

Considering various external heat fluxes and oxygen contents, the limits of the range of strain rates where a diffusion flame can be sustained vary substantially. At the limits of this range, two different extinction modes are identified and investigated separately. Blow-off at high strain rates occurs under all investigated conditions. The associated critical Damköhler number decreases slightly when increasing the magnitude of the external incident heat flux, and decreases more

significantly when increasing the oxygen content. Quenching at low strain rates is only found for positive values of Ω, where the associated critical Damköhler number increases when increasing either the external incident heat flux or the oxygen content. For negative values of Ω, the flame can be theoretically sustained even at infinitely low strain rates.

Furthermore, from the theoretical model, it was found that the occurrence of quenching depends not only on the oxygen content but also on the magnitude of the external incident heat flux, that determines the radiative exchange at that char layer. This new multi-variable dependency of extinction conditions strongly challenges the sole use of the magnitude of the external incident heat flux as a surrogate to define the occurrence of self-extinction in fire safety engineering design.

The theoretical results obtained were contrasted with experimental data obtained through bench-scale experiments conducted using timber samples in different oxygen contents and under a range of external radiative heat fluxes. The evaluation of the experimental critical Damköhler number at quenching shows the same behavior exhibited by the theoretical results for positive values of Ω but with a lower sensitivity to the testing parameters.

To account for discrepancies between the theoretical and experimental sensitivity to oxygen content and external heat flux variations, a fuel dilution parameter is introduced. Fuel dilution is considered as a simple way to model the complex variations of timber decomposition and surface reactions with the ambient conditions. This parameter shall be further investigated in future work, given the good agreements between experimental and theoretical quenching conditions once it is considered.

5 Acknowledgments

The authors would like to recognize the support of CONICYT-Becas Chile (Grant No. 2016-72170283) and the Australian Research Council Hub for Advanced Solutions to Transform Tall Timber Buildings (Grant No. IH150100030).

References

[1] I.S. Wichman, A. Atreya, A simplified model for the pyrolysis of charring materials, Combust. Flame. 68 (1987) 231–247.

[2] A.F. Roberts, Calorific values of partially decomposed wood samples, Combust. Flame. 8 (1964) 245–246.

[3] G. Lake, K. Rathbone, P. Vivian, K. Whittle, Case Study Shaping Australia's Tall Tower Design And High Livability Standards, Counc. Tall Build. Urban Habitat J. 4 (2017) 12–19.

[4] E. Zukoski, Fluid Dynamic Aspects Of Room Fires, Fire Saf. Sci. 1 (1986) 1–30.

[5] G. Heskestad, Fire plume air entrainment according to two competing assumptions, Symp. (Int.) Combust. 21 (1988) 111–120.

[6] R. Emberley, T. Do, J. Yim, J.L. Torero, Critical heat flux and mass loss rate for extinction of flaming combustion of timber, Fire Saf. J. 91 (2017) 252–258.

[7] A. Bartlett, R. Hadden, L. Bisby, B. Lane, Auto-extinction of engineered timber: the application of firepoint theory, in: Interflam, 2016.

[8] R. Crielaard, J.W. van de Kuilen, K. Terwel, G. Ravenshorst, P. Steenbakkers, Self-extinguishment of cross-laminated timber, Fire Saf. J. 105 (2019) 244–260.

[9] J. Cuevas, J.L. Torero, C. Maluk, Flame extinction and burning behaviour of timber under varied oxygen concentrations, Fire Saf. J. 120 (2020).

[10] R. Emberley, A. Inghelbrecht, Z. Yu, J.L. Torero, Self-extinction of timber, Proc. Combust. Inst. 36 (2017) 3055–3062.

[11] V. Gupta, J.L. Torero, J.P. Hidalgo, Burning dynamics and in-depth flame

spread of wood cribs in large compartment fires, Combust. Flame. 228 (2021) 42–56.

[12] R. Emberley, C. Gorska Putynska, A. Bolanos, A. Lucherini, A. Solarte, D. Soriguer, M. Gutierrez Gonzalez, K. Humphreys, J.P. Hidalgo, C. Maluk, A. Law, J.L. Torero, Description of small and large-scale cross laminated timber fire tests, Fire Saf. J. 91 (2017) 327–335.

[13] D.J. Rasbash, D.D. Drysdale, D. Deepak, Critical heat and mass transfer at pilot ignition and extinction of a material, Fire Saf. J. 10 (1986) 1–10.

[14] A.I. Bartlett, R.M. Hadden, J.P. Hidalgo, S. Santamaria, F. Wiesner, L.A. Bisby, S. Deeny, B. Lane, Auto-extinction of engineered timber: Application to compartment fires with exposed timber surfaces, Fire Saf. J. 91 (2017) 407–413.

[15] J. Cuevas, J.P. Hidalgo, J.L. Torero, C. Maluk, Complexities of the Thermal Boundary Conditions when Testing Timber using the Fire Propagation Apparatus, in: Proc. Ninth Int. Semin. Fire Explos. Hazards, St. Petersburgh, Rusia, 2019: pp. 959–969.

[16] F.E. Fendell, Ignition and extinction in combustion of initially unmixed reactants, J. Fluid Mech. 21 (1965) 281–303.

[17] L. Krishnamurthy, F.A. Williams, K. Seshadri, Asymptotic theory of diffusion-flame extinction in the stagnation-point boundary layer, Combust. Flame. 26 (1976) 363–377.

[18] F. A. Williams, Combustion theory, CRC Press, Boca Raton, USA, 1985.

[19] A. Liñán, The asymptotic structure of counterflow diffusion flames for large activation energies, Acta Astronaut. 1 (1974) 1007–1039.

[20] B.H. Chao, C.K. Law, Asymptotic theory of flame extinction with surface radiation, Combust. Flame. 92 (1993) 1–24.

[21] J. Quintiere, Fundamentals of Fire Phenomena, John Wiley & Sons, Ltd,

Chichester, UK, 2006.

[22] S.H. Sohrab, A. Liñán, F.A. Williams, Asymptotic Theory of Diffusion-Flame Extinction with Radiant Loss from the Flame Zone, Combust. Sci. Technol. 27 (1982) 143–154.

[23] B.H. Chao, C.K. Law, J.S. T'ien, Structure and extinction of diffusion flames with flame radiation, Symp. (Int.) Combust. 23 (1991) 523–531.

[24] A.F. Roberts, G. Clough, Thermal decomposition of wood in an inert atmosphere, Symp. (Int.) Combust. 9 (1963) 158–166.

[25] D.J. Rasbash, B. Langford, Burning of wood in atmospheres of reduced oxygen concentration, Combust. Flame. 12 (1968) 33–40.

[26] M. Kleiber, R. Joh, VDI Heat Atlas, Springer Berlin Heidelberg, Berlin, Heidelberg, 2010.

[27] J. Li, Z. Zhao, A. Kazakov, M. Chaos, F.L. Dryer, J.I. Scire, A comprehensive kinetic mechanism for CO, CH2O, and CH 3OH combustion, Int. J. Chem. Kinet. 39 (2007) 109–136.

[28] D. Drysdale, An introduction to fire dynamics : 3rd ed., Wiley, Chichester, West Sussex, 2011.

[29] C. Branca, C. Di Blasi, Global Kinetics of Wood Char Devolatilization and Combustion, Energy & Fuels. 17 (2003) 1609–1615.

[30] P. Boulet, D. Brissinger, A. Collin, Z. Acem, G. Parent, On the influence of the sample absorptivity when studying the thermal degradation of materials, Materials (Basel). 8 (2015) 5398–5413.

[31] R. Emberley, Fundamentals for the Fire Design of Cross Laminated Timber Buildings, The University of Queensland, 2017.

[32] M. Spearpoint, J. Quintiere, Predicting the burning of wood using an integral model, Combust. Flame. 123 (2000) 308–325.

[33] S.R. Turns, An Introduction to Combustion: Concepts and Applications, 2nd

ed., McGraw-Hill, Singapore, 2000.

[34] H.G. Im, J.K. Bechtold, C.K. Law, Counterflow Diffusion Flames with Unsteady Strain Rates, Combust. Sci. Technol. 106 (1995) 345–361.

[35] J.L. Torero, T. Vietoris, G. Legros, P. Joulain, Estimation of a total mass transfer number from the standoff distance of a spreading flame, Combust. Sci. Technol. 174 (2002) 187–203.

[36] F. Browne, Theories of the combustion of wood and its control, United States Dep. Agric. For. Serv. Rep. No. 2136. (1958) 1–72.

[37] M.N. Belgacem, A. Pizzi, eds., Lignocellulosic fibers and wood handbook, Scrivener Publishing LLC., Beverly, MA, 2016.

[38] G. Rein, Smouldering Combustion Phenomena in Science and Technology, Int. Rev. Chem. Eng. 1 (2009) 3–18.

[39] T.J. Ohlemiller, Smoldering combustion propagation through a permeable horizontal fuel layer, Combust. Flame. 81 (1990) 341–353.